Reference: *Biol. Bull.* **207:** 1–16. (August 2004)
© 2004 Marine Biological Laboratory

Propagation and Perception of Bioluminescence: Factors Affecting Counterillumination as a Cryptic Strategy

SÖNKE JOHNSEN[1,*], EDITH A. WIDDER[2], AND CURTIS D. MOBLEY[3]

[1]*Biology Department, Duke University, Durham, North Carolina 27708;*
[2]*Marine Science Division, Harbor Branch Oceanographic Institution, Ft. Pierce, Florida 34946; and* [3]*Sequoia Scientific Inc., Bellevue, Washington 98005*

Abstract. Many deep-sea species, particularly crustaceans, cephalopods, and fish, use photophores to illuminate their ventral surfaces and thus disguise their silhouettes from predators viewing them from below. This strategy has several potential limitations, two of which are examined here. First, a predator with acute vision may be able to detect the individual photophores on the ventral surface. Second, a predator may be able to detect any mismatch between the spectrum of the bioluminescence and that of the background light. The first limitation was examined by modeling the perceived images of the counterillumination of the squid *Abralia veranyi* and the myctophid fish *Ceratoscopelus maderensis* as a function of the distance and visual acuity of the viewer. The second limitation was addressed by measuring downwelling irradiance under moonlight and starlight and then modeling underwater spectra. Four water types were examined: coastal water at a depth of 5 m and oceanic water at 5, 210, and 800 m. The appearance of the counterillumination was more affected by the visual acuity of the viewer than by the clarity of the water, even at relatively large distances. Species with high visual acuity (0.11° resolution) were able to distinguish the individual photophores of some counterilluminating signals at distances of several meters, thus breaking the camouflage. Depth and the presence or absence of moonlight strongly affected the spectrum of the background light, particularly near the surface. The increased variability near the surface was partially offset by the higher contrast attenuation at shallow depths, which reduced the sighting distance of mismatches. This research has implications for the study of spatial resolution, contrast sensitivity, and color discrimination in deep-sea visual systems.

Received 15 December 2003; accepted 17 April 2004.

* To whom correspondence should be addressed. E-mail: sjohnsen@duke.edu

Abbreviations: MTF, modulation transfer function; OTF, optical transfer function; PSF, point spread function.

Introduction

Counterillumination is a common form of crypsis in the open ocean (Latz, 1995; Harper and Case, 1999; Widder, 1999). Its prevalence is due to the fact that, because the downwelling light is orders of magnitude brighter than the upwelling light, even an animal with white ventral coloration appears as a black silhouette when viewed from below (Johnsen, 2002). This is particularly disadvantageous because an object is detectable at a far greater distance when viewed from below than when viewed from any other angle (Mertens, 1970; Johnsen, 2002). Aside from extremely transparent tissue, which is not easy to achieve in larger species with complex tissues, the way to overcome this disadvantage is for the ventral surface to emit light that matches the downwelling light in intensity, spectrum, and angular distribution. Indeed, this solution is nearly ubiquitous in nontransparent mesopelagic species, particularly in crustaceans, fish, and squid (Young and Roper, 1976; Herring, 1977, 1985; Widder, 1999).

Counterilluminating species have evolved complex strategies to match the intensity, spectrum, and angular distribution of the downwelling light (Denton *et al.*, 1972; Young and Mencher, 1980; Herring, 1983; Widder, 1999). One aspect that is poorly understood, however, is the spatial distribution of the photophores (Young and Roper, 1976). While some species (*e.g.*, the cookie cutter shark *Isistius*

brasiliensis) have many small photophores that evenly illuminate the ventral surface, most have a smaller number of isolated photophores that produce uneven illumination (*e.g.*, Fig. 2d). Thus, even if the photophores match the spectrum and intensity of the downwelling light perfectly, the counterilluminator will be visible when viewed at a distance that allows these individual sources to be discerned. To investigate this problem, the effects of the intervening water and the viewer's visual acuity on the perceived image of the counterillumination must be understood.

This study examines the effects of underwater light scattering and visual acuity on the perceived images of counterillumination signals. The effects are modeled with Monte Carlo methods and image transfer theory, using data collected from water types ranging from shallow coastal water to the deep mesopelagic zone (800 m). Three visual systems, with high, medium, and low acuity, are also examined. The goal is to determine under which conditions counterilluminators are still visible and what implications this has for both camouflage and visual detection under low-light conditions.

Materials and Methods

General principles of image transfer

The perceived image of a counterilluminating animal viewed from a distance is affected by three factors: absorption and scattering by the water and the acuity of the viewer's eye. The water and associated particulates potentially dim and blur the image, and the acuity of the eye determines the resolution of the perceived image.

The effect of the first factor is generally modeled in the following way. First, the optical effects of the water on the image of a point source are calculated. The image of a point source is known as the point spread function (PSF) (Mertens and Replogle, 1977). The point source is then convolved with a given image to determine the appearance of the image after it passes through the water. In a convolution, each point in the image is replaced by its product with the point spread function (Fig. 1). Fortunately, this computationally expensive procedure can be streamlined using the convolution theorem, which states that for any two images I_1 and I_2, the convolution of I_1 with I_2 is equal to the inverse Fourier transform of the product of the Fourier transforms of the two images: that is,

$$I_1 * I_2 = \mathcal{F}^{-1}[\mathcal{F}(I_1) \cdot \mathcal{F}(I_2)], \quad \text{(Fig. 1)} \quad \text{(Equation 1)}$$

where * denotes convolution, and $\mathcal{F}(I)$ and $\mathcal{F}^{-1}(I)$ are the Fourier and inverse Fourier transforms of an image I (Goodman, 1996). Let I_1 be the image of the counterillumination, and I_2 be the point spread function. Substituting into equation (1) gives

$$\text{image} * \text{PSF} = \mathcal{F}^{-1}[\mathcal{F}(\text{image}) \cdot \mathcal{F}(\text{PSF})]. \quad \text{(Equation 2)}$$

The Fourier transform of the point spread function is gen-

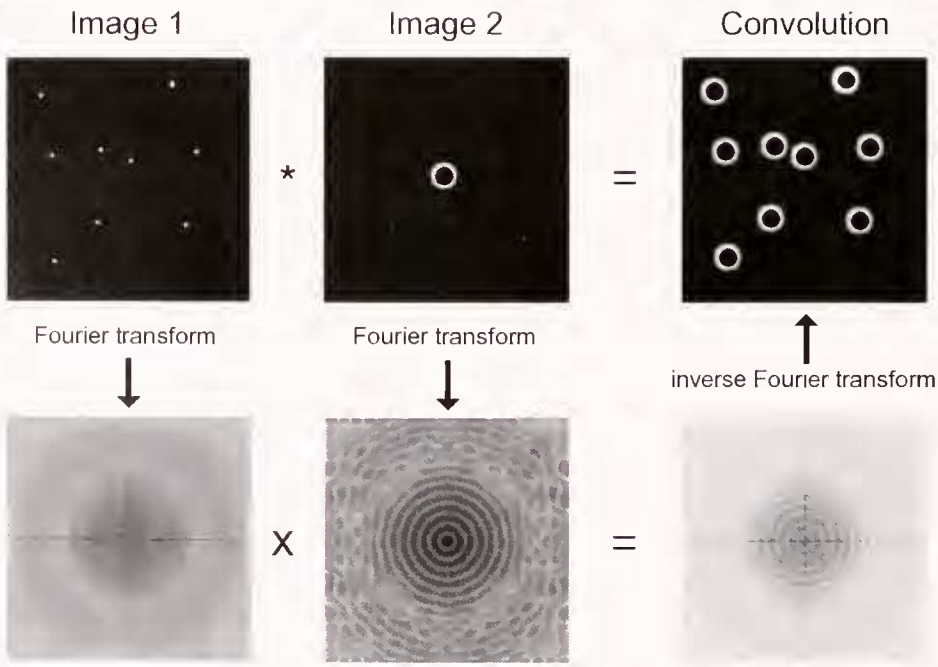

Figure 1. The convolution of image 1 and image 2 (denoted by the "*" operator) can be calculated by multiplying the Fourier transforms of the two images and then calculating the inverse Fourier transform of the product.

erally referred to as the optical transfer function (OTF). Due to the convolution theorem, the OTF of a whole system is simply the product of the OTFs of the various components in the system (Goodman, 1996). Thus, for this study

$$\text{image}_{\text{final}} = \mathcal{F}^{-1}[\mathcal{F}(\text{image}_{\text{initial}}) \cdot \text{OTF}_{\text{water}} \cdot \text{OTF}_{\text{eye}}], \qquad \text{(Equation 3)}$$

where $\text{image}_{\text{final}}$ is the perceived image and $\text{OTF}_{\text{water}}$ and OTF_{eye} are the optical transfer functions of the water and eye respectively. A final, convenient implication of the convolution theorem is that the OTF of x meters of optically homogeneous water is equal to the OTF of 1 meter of water to the xth power. Thus, one need only calculate the PSF for one distance. This property, known as the linearity assumption, does not hold in extreme cases (*e.g.*, very large x), but is appropriate for the situations examined in this study (Jaffe, 1992). The equation for underwater image transfer is then

$$\text{image}_{\text{final}}(x) = \mathcal{F}^{-1}[\mathcal{F}(\text{image}_{\text{initial}}) \cdot (\text{OTF}_1)^x \cdot \text{OTF}_{\text{eye}}], \qquad \text{(Equation 4)}$$

where $\text{image}_{\text{final}}(x)$ is the perceived image viewed from a distance of x meters, and OTF_1 is the optical transfer function of the water over a distance of 1 meter.

Although Eq. (4) correctly describes the propagation of a two-dimensional image, it requires modification when used in the context of counterillumination, because the background radiance is affected by the entire three-dimensional light field and changes as the viewer moves down and away from its target. From Mertens (1970), the degradation of contrast of a large image underwater (*i.e.*, the OTF at zero spatial frequency) is

$$\text{OTF}(0) = \frac{C_x}{C_0} = e^{-(c-K_L)x}, \qquad \text{(Equation 5)}$$

where C_x and C_0 are contrast at x and 0 meters viewing distance, c is the beam attenuation coefficient, and K_L is the attenuation coefficient of the background radiance. In the case of upward viewing, K_L equals K_{Ld}, the attenuation coefficient of direct downward radiance (Johnsen, 2002).

The correct OTF for objects being viewed from below is obtained by normalizing the original OTF so that OTF(0) equals $e^{-(c-K_{Ld})x}$ (Mertens, 1970). Thus the final equation for the propagation of images viewed from below is

$$\text{image}_{\text{final}}(x) = \mathcal{F}^{-1}\left[\mathcal{F}(\text{image}_{\text{initial}}) \cdot \left(e^{-(c-K_{Ld})} \cdot \frac{\text{OTF}_1}{\text{OTF}_1(0)}\right)^x \cdot \text{OTF}_{\text{eye}}\right]. \qquad \text{(Equation 6)}$$

The OTF is a complex-valued function and difficult to interpret. Therefore, its magnitude, known as the modulation transfer function (MTF), is often also calculated. The MTF is quite useful because it gives the fraction of remaining image contrast as a function of spatial frequency. For example, MTF(4) = 0.5 implies that 50% of the original image contrast remains for detail that has a spatial frequency of 4 cycles per degree.

Images examined

Images of the ventral bioluminescence of two counterilluminating species were used: (1) the enoploteuthid squid *Abralia veranyi* (Rüppell, 1844) (eye-flash squid), and (2) the myctophid fish *Ceratoscopelus maderensis* (Gunther, 1864) (horned lanternfish) (Fig. 2A, B). The two were chosen to provide a range of photophore spacing. Counterillumination in *A. veranyi* is finely detailed; that of *C. maderensis* is relatively coarse (Fig. 2C, D). *A. veranyi* was collected at depth, using the *Johnson-Sea-Link* research submersible fitted with 11-liter acrylic plastic cylinders with hydraulically activated, sliding lids. *C. maderensis* was collected at night, using an opening/closing Tucker trawl (4.3-m^2 opening, ¼ inch knotless nylon mesh) fitted with a thermally insulated collecting container. Specimens were manually stimulated to bioluminesce, and then were recorded with a Dage ISIT image-intensified video camera (*A. veranyi*) or Intevac GenIISys image intensifier system and CCD video camera (*C. maderensis*). Images that show how the counterilluminating animals appear from below (Fig. 2E, F) were created by combining the bioluminescence images with silhouettes of the animals obtained from normal illumination photographs (taken immediately after the intensified images). Non-illuminating portions of the animals are shown as black because this is how they appear against the downwelling light (Johnsen, 2002). The natural posture of *A. veranyi* is unknown. Although observers in submersibles generally find mesopelagic squid with their fins folded and their arms and tentacles placed over their heads (Vecchione and Roper, 1991; Fig. 2A), this is may be a response to the perceived threat from the submersible. In the silhouette chosen, the fins and appendages were extended to examine their effect on visibility.

The backgrounds were set to a brightness equal to the average brightness of the counterilluminating animal (minus the fins, arms, and tentacles in the case of the squid). Because these relative values allow the animal to blend with the background most easily, it is assumed that they approximately match what would be observed in the field. The backgrounds for the *C. maderensis* images are darker because the average brightness of the animal is darker (due to the wider spacing of the photophores). Note that these figures show *relative* brightnesses, chosen to maximize visibility on the printed page. The *absolute* brightnesses are of

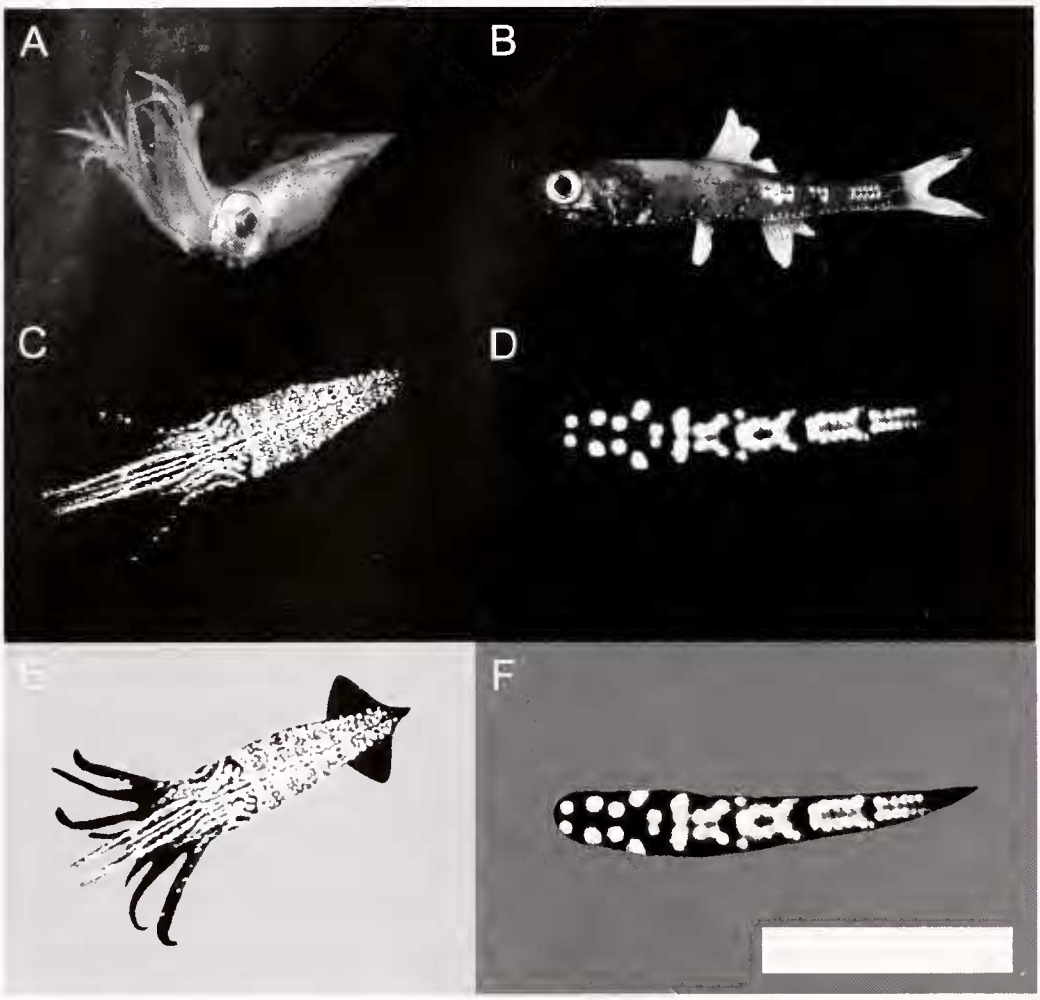

Figure 2. (A) The eye-flash squid *Abralia veranyi*. (B) The horned lanternfish *Ceratoscopelus maderensis*. (C) Counterillumination of *A. veranyi*. (D) Counterillumination of *C. maderensis*. (E) Counterillumination of *A. veranyi* as viewed from below against the downwelling light. (F) Counterillumination of *C. maderensis* as viewed from below against the downwelling light. Scale bar is 5 cm. Background in (E) and (F) is set to the average brightness of the counterilluminating animal. Panel B courtesy of Marine Biological Laboratory Digital Archive, Flescher Fish Collection.

course much dimmer (far beyond the reach of printed paper) and can only be seen by the dark-adapted eye.

The intensified images are not perfect representations of the actual counterillumination. The resolution of the images is low, and the photophore signals are slightly expanded due to "blooming" of the image at the detector array. In addition, although counterillumination is more stable than other bioluminescent signals, the images are static representations of potentially variable light emission. Indeed, a subset of the ventral photophores in *A. veranyi* was not lit in the studied image (Herring *et al.*, 1992). This relatively low number of small photophores most likely would not change a spatial distribution that is already quite uniform. However, they may play a role in spectral changes. In *C. maderensis*, all the ventral photophores were emitting during the image exposure.

Calculation of point spread functions and attenuation coefficients

The PSFs in this study were determined using Monte Carlo software (BSFPSF ver. 1.1., developed by CDM). Five million simulated photons were tracked from an isotropic point source (of unit power) to their point of intersection with a sphere of radius 1 m. Although a PSF is defined as the image of a cosine point source, the use of an isotropic point source achieves the same result because scattering in natural waters is primarily in a forward direction (Mertens and Replogle, 1977; confirmed by preliminary calculations). Due to the symmetry of an isotropic point source, calculations could be completed in far less time than if a cosine point source were used.

The radiance distribution of the simulated photons at the

intersection with the 1-m sphere is the PSF. The three factors (besides distance) affecting the PSF are (1) the absorption coefficient a, (2) the scattering coefficient b, and (3) the phase function γ. The first and second factors specify how often a photon is absorbed or scattered by the water and associated particulates. The third factor specifies the angular distribution of the scattered light. Absorption and attenuation coefficients were obtained for four water types: (1) coastal water at 5-m depth, (2) oceanic water at 5-m depth, (3) oceanic water at 210-m depth, and (4) oceanic water at 800-m depth (Table I). Absorption and scattering coefficients for coastal water were obtained by Dr. Heidi Sosik (Woods Hole Oceanographic Institution, Woods Hole, MA) using a dual-path, multiband absorption/attenuation meter (ac-9, WETLabs Inc.) at a site 80 km from the coast of Portsmouth, New Hampshire (42°47′N 70°05′W, 1106 local time, 30 June 2000) (see Johnsen and Sosik, 2003, for details). Optical coefficients in oceanic water (Jerlov type I) at 5 m and 210 m were obtained by Drs. Andrew Barnard, Scott Pegau, and Ronald Zaneveld (College of Oceanic and Atmospheric Sciences, Oregon State University, Corvallis, Oregon) using the same equipment in the equatorial Pacific (1005 local time, 30 April 1996; 0°0′N 177°21′W). Optical coefficients in oceanic water at 800-m depth were obtained from Capone *et al.* (2002). In all cases, absorption and beam attenuation coefficients were measured at 412, 440, 488, 510, 532, 555, 650, and 676 nm. Although point spread functions were calculated for all eight wavelengths, for clarity only those at 412, 488, 555, and 650 nm are analyzed and discussed in this study. While the 5-m coastal measurement is somewhat specific to measurement site, the three oceanic measurements are typical of most oceanic waters, particular those at 210 and 800 m.

Because the ac-9 absorption-attenuation meter has detectors of finite size, light scattered over small angles was collected by the detector and incorrectly interpreted as unscattered. Thus, scattering was underestimated by a small amount. If one assumes that the scattering matches Petzold's phase function, then the scattering coefficient is underestimated by approximately 20%. Again, preliminary results showed that this had negligible effect on the blurring of the image, though it would have resulted in slightly greater attenuation of the contrast of the whole image. The ac-9 meter also does not measure certain factors that may influence image propagation, such as marine snow and refractive index inhomogeneities. The large particles of marine snow will limit the long-range visibility of small objects by direct occlusion, and refractive index inhomogeneities may slightly increase scattering at very small angles (below the resolution limit of the visual systems examined) (Bogucki *et al.*, 1998).

The phase function γ was chosen to be the commonly used "average particle" function (Mobley *et al.*, 1993) based on measurements by Petzold (1977). In productive coastal waters, most of the light is scattered by living phytoplankton, which have a backscatter fraction of 0.01 or less (*e.g.*, Ulloa *et al.*, 1994). However, in clear oceanic water, isotropic scattering by the water itself is a significant fraction of the total scattering, and the total backscatter fraction can be as large as 0.04 (Mobley, 1994). We chose Petzold's average particle phase function (Mobley *et al.*, 1993), which has a backscatter fraction of 0.018, about midway between the two extremes. Preliminary results showed that, because scattered light was extremely dim compared to the unscattered direct beam, the choice of phase function made no notable difference.

PSF values were calculated up to 10°, at 0.05° intervals. Although the PSF from 0 to 1° was calculated using Monte Carlo methods, computational limits (due to the small size of the angular bins receiving scattered photons) prevented accurate calculations at substantially higher angles for the given number of initial photons. Therefore, the PSF from 1° to 10° was estimated by fitting the PSF from 0.45° to 1° to a power function and then extrapolating by 0.05° increments up to an angle of 10° (see Voss, 1991, for justification).

The optical transfer functions of the eyes were modeled as the Gaussian curve:

$$\mathrm{OTF}(\nu) = e^{-3.56\cdot(R\nu)^2} \qquad \text{(Equation 7)}$$

where ν is the spatial frequency (in cycles/degree) and R is the spatial resolution (Warrant, 1999). This function, often used to model the OTF of visual systems, results in a barely

Table I

Absorption and scattering coefficients (a and b respectively) used in the Monte Carlo calculation of point spread functions

Wavelength (nm)	Coastal water at 5-m depth		Oceanic water at 5-m depth		Oceanic water at 210-m depth		Oceanic water at 800-m depth	
	a	*b*	*a*	*b*	*a*	*b*	*a*	*b*
412	0.29	0.26	0.035	0.11	0.060	0.018	0.027	0.020
488	0.15	0.21	0.038	0.098	0.035	0.013	0.027	0.014
555	0.11	0.19	0.073	0.091	0.077	0.0094	0.072	0.0060
650	0.37	0.15	0.36	0.085	0.36	0.014	0.36	0.014

detectable contrast of 2.8% ($= e^{-3.56}$) at the spatial resolution of the eye. The spatial resolutions of three mesopelagic fish were chosen to span a wide range of visual acuity: (1) $R = 0.11°$ (the "lovely hatchetfish" *Argyropelecus aculeatus*), (2) $R = 0.23°$ (the spookfish *Opisthoproctus soleatus*), and (3) $R = 0.50°$ (the myctophid fish *Lampanyctus festivus*) (Collin *et al.*, 1997; Wagner *et al.*, 1998). *A. aculeatus* and *O. soleatus* both have upward-viewing tubular eyes; *L. festivus* has lateral-viewing eyes and so probably does not search for overhead, counterilluminating prey.

The acuity of these species was measured from the density of their retinal ganglion cells (which accounts for spatial summation). Because these counts also include displaced ganglion cells, they may slightly overestimate acuity. The predicted acuity also assumes a well-focused image, but this is generally the case for the foveal regions of deep-sea eyes (Warrant and Locket, 2004). Increasing spatial summation will also lower the acuity. Finally, it is important to note that these spatial resolutions do not include potential blurring of a moving image due to large temporal summation. Since long temporal summation times are common at depth (Frank, 1999) and animals do drift relative to one another in the water, the actual spatial resolution in certain situations may be less than that predicted by retinal morphology.

The minimum contrast threshold is the smallest percentage variation in radiance that can be detected. This value for fish is approximately 1%–2% in bright light, but it rises as depth increases (Douglas and Hawryshyn, 1990). Though few direct measurements have been made, the threshold at mesopelagic light levels appears to range from about 25% to 50% (*e.g.*, threshold for the Atlantic cod *Gadus morhua* at 650-m depth is approximately 50% (Anthony, 1981)). We therefore set the minimum contrast threshold at 33%, while accepting that depth, water clarity, and special visual adaptations make the actual threshold highly variable.

The attenuation coefficients of direct downward radiance K_{Ld} were calculated by modeling the underwater radiance distribution using radiative transfer software (Hydrolight 4.2, Sequoia Scientific Inc., Bellevue, WA, www.hydrolight.info). The inherent optical properties required by the software were obtained from measured vertical profiles of chlorophyll concentration and absorption and scattering coefficients from the four water types examined (see Johnsen, 2002; and Johnsen and Sosik, 2003, for details). The sun was assumed to be at the zenith on a clear day with no wind.

Measurement of moonlight and starlight spectra

Nocturnal spectra under moonlight and starlight were measured using a spectrometer with a highly sensitive photomultiplier detector (OL-754-PMT, Optronics Laboratories Inc., Orlando, FL). Moonlight spectra were measured in air on a barrier island in Florida during full moon (moon was at its peak elevation). An integrating sphere was used to collect light from all regions of the sky. Starlight spectra were measured on a moonless night on a completely darkened ship in the center of the Gulf Stream (latitude ~27°N) to ensure a complete absence of light pollution. To minimize light loss, the integrating sphere was removed and the entrance slit of the spectrometer (~30° angular field) was aimed at the zenith. The downwelling irradiance at 5-m depth under moonlight and starlight was calculated using the above-described radiative transfer software, with the correct skylight spectrum as an input.

Results

Point spread and optical transfer functions of the water types and visual resolutions

The point spread functions in all four water types were extremely narrow, with the radiance at zero degrees 2–3 orders of magnitude larger than the radiance at higher angles (at a distance of 5 m) (Fig. 3). With increasing water clarity and depth, this effect became more pronounced. The wavelength dependence of the PSF was complex, depending on the relative numbers of scattering and absorption events.

In all four water types, the modulation transfer function was primarily affected by the visual resolution of the viewer's eye (Fig. 4). However, the MTFs in near-surface waters decreased at higher spatial frequencies (independently of the decrease due to visual acuity limitations), indicating some blurring by the water (Fig. 4A, B). The MTFs within a given water type had similar shapes and differed primarily in magnitude (set by $\mathrm{MTF}(0) = e^{-5(c - K_{Ld})}$). This magnitude had a complicated wavelength dependence, being proportional to wavelength in near-surface waters and inversely proportional to wavelength in deep waters.

Perceived images

The perceived images were dramatically affected by the visual resolution of the viewer and, to a lesser extent, by scattering and absorption by the water (Figs. 5, 6). When viewed at 0.11° resolution, *Ceratoscopelus maderensis* and *Abralia veranyi* had a contrast greater than 33% at distances up to 4 to 8 m (though the visibility of the latter was primarily due to the unlit fins and appendages). However, when viewed at 0.5° resolution, the contrast of the counterillumination was greater than 33% only up to a distance of 1 to 2 m. The individual photophores of *C. maderensis* were distinguishable up to 2 m at 0.11° resolution, and the general pattern of photophores was distinguishable up to 2 m at lower resolutions. The general pattern of the photophores of

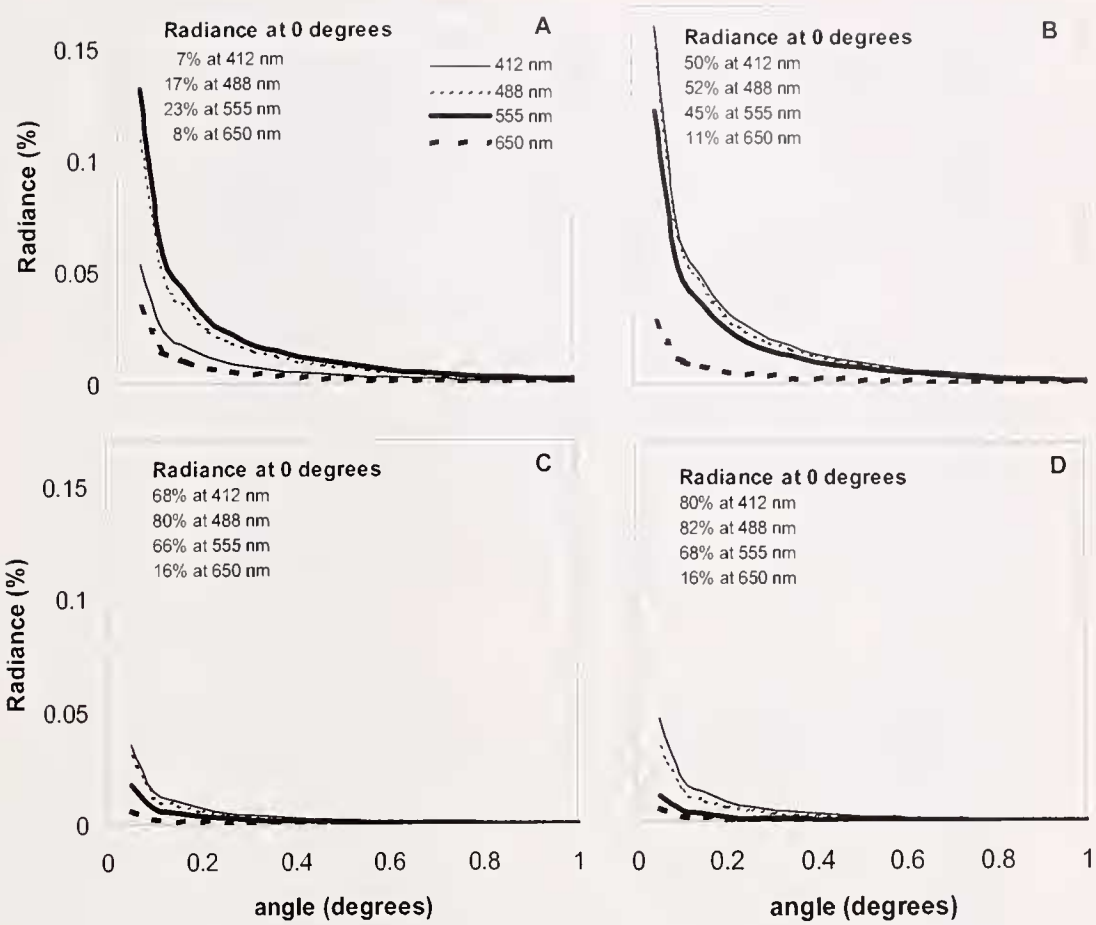

Figure 3. Radiance *vs.* angle for a point source viewed from a distance of 5 m (point spread function). The radiance is normalized by the radiance of a point source viewed at 5 m in a medium that does not scatter or absorb light. (A) Coastal water at 5-m depth. (B) Oceanic water at 5-m depth. (C) Oceanic water at 210-m depth. (D) Oceanic water at 800-m depth. The normalized radiances at zero degrees are given numerically rather than graphically because they are far higher than the other values.

A. veranyi was evident at 1 m at 0.11° resolution, but not at lower resolutions.

The counterillumination of both species is visible at roughly twice the distance in the clearest conditions studied (at 488 nm in oceanic water at 800-m depth) as it is in the most turbid conditions (at 412 nm in coastal water at 5-m depth) (Fig. 5A *vs.* 5B, Fig. 6A *vs.* 6B). The difference was entirely due to the difference in MTF(0) between the two water types (95% *vs.* 37% at a distance of 5 m) and not to significantly increased blurring of fine detail.

Variation of background spectra and wavelength dependence of contrast attenuation

The background spectra at shallow depths under moonlight and starlight differed substantially in both coastal and oceanic waters, particularly at shorter wavelengths (Fig. 7A, B). Under starlight, the spectrum narrowed and the peak wavelength was long-shifted (by 40 to 80 nm depending on the water type and what is considered the true peak). The background spectra were also affected substantially by depth, even at mesopelagic depths. As the depth increased from 200 to 800 m, the spectra of the downwelling irradiance narrowed slightly and the peak wavelength shifted from 490 nm to 480 nm (Fig. 7C).

General contrast attenuation was relatively rapid and wavelength-independent at 5-m depth in both coastal and oceanic waters, with sighting distances (proportional to $1/c - K_{Ld}$) only 5%–20% of those in deeper waters (Fig. 7D). At greater depths, sighting distance was highly dependent on wavelength. At these depths, sighting distance increased with wavelength, until it reached a peak at a wavelength about 30 nm longer than that of the peak wavelength of downwelling irradiance. After this peak, the sighting distance decreased rapidly with wavelength. For wavelengths greater than 600 nm, the sighting distances at depth were less than those near the surface.

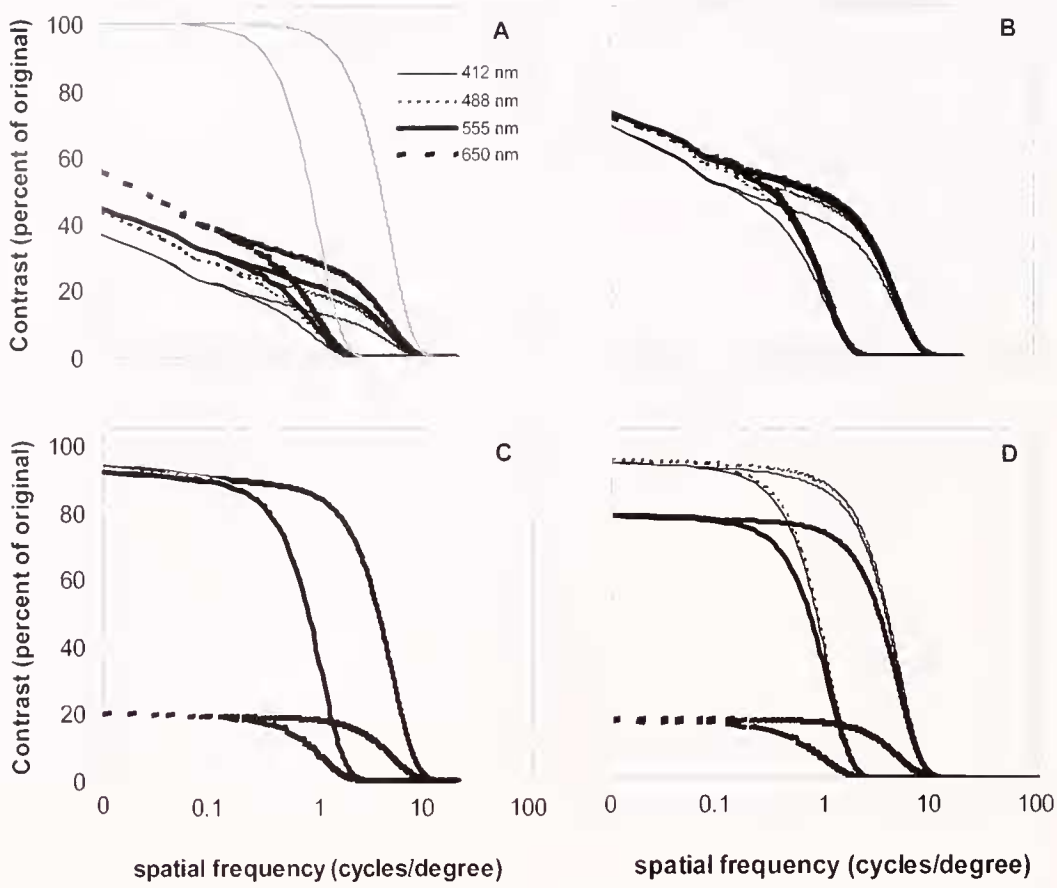

Figure 4. Contrast as a function of spatial frequency for an object viewed from a distance of 5 m (modulation transfer function, MTF). The contrast is normalized by the contrast at a distance of 0 m. (A) Coastal water at 5-m depth. (B) Oceanic water at 5-m depth. (C) Oceanic water at 210-m depth. (D) Oceanic water at 800-m depth. The MTF is shown for two visual systems, one with 0.11° resolution and one with 0.5° resolution. At a spatial frequency of approximately 0.4 cycles/deg, the data split, with the lower trace denoting 0.5° resolution. The two gray lines in (A) denote the MTF for the eyes alone. Because the MTF at 0 cycles/deg is important, the graphs include this point despite being logarithmic.

Discussion

This study shows that a counterilluminating individual faces a number of difficulties. First, an acute eye (0.11° resolution) with moderate contrast sensitivity (33%) can detect the photophore patterns of both *Abralia veranyi* and *Ceratoscopelus maderensis* at distances greater than 1 m. Second, even the water at the relatively turbid shallow coastal site blurred the counterillumination signals very little. Although all four water types did lower the overall contrast of the counterilluminator, the attenuation rate was quite low, particularly at mesopelagic (>200 m) depths. Finally, the spectrum of downwelling background light varied considerably with depth in the mesopelagic zone and was strongly affected by the source of nocturnal illumination at the shallow depths. This suggests that counterilluminating photophores must be spaced closely together when viewed by visually acute species, and that matching the background spectrum may be more difficult than previously considered. From the predator's point of view, this study suggests that high spatial resolution and color discrimination in the blue-green portion of the spectrum are highly advantageous for detecting counterilluminating prey. However, since both of these characteristics reduce sensitivity, they also have a cost that must be balanced.

The remainder of the paper explores these limitations in detail. It is important to note that, despite these limitations, counterillumination dramatically decreases the visibility of the individual. The visibility of *A. veranyi* at distances greater than 1 m is entirely due to the unlit fins, tentacles, and arms (Fig. 5), which may be held above and against the body to minimize their silhouette (Fig. 2A). The visibility of these unlit regions at distances of at least 8 m highlights the impressive crypsis afforded by counterillumination. In addition, in certain cases the goal may not be complete cryp-

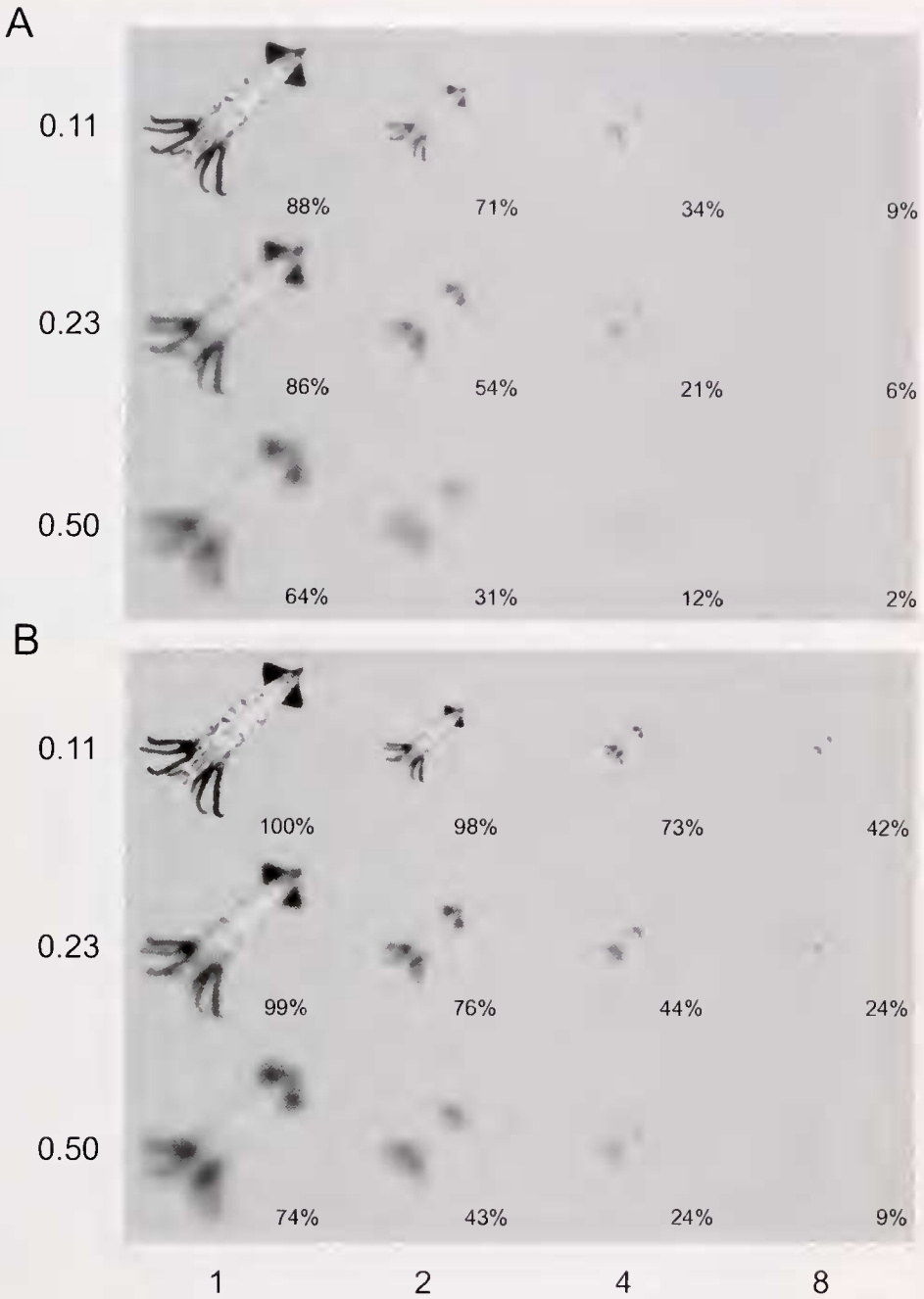

Figure 5. Counterillumination of *Abralia veranyi* viewed from distances of 1, 2, 4, and 8 m by animals with eyes of 0.11°, 0.23°, and 0.5° resolution. (A) Counterillumination is viewed at a wavelength of 412 nm in coastal water at 5-m depth (the optical conditions that had the greatest effect on image propagation). (B) Counterillumination is viewed at a wavelength of 488 nm in oceanic water at 800-m depth (the optical conditions that had the least effect on image propagation). The percentages indicate the maximum contrast in each image. All images are scaled in size for viewing distance, and the backgrounds are all set equal. To see the absolute brightness values in the image, view the figure under dim illumination so that the printed background matches the brightness at the relevant depth. For example, to see what the counterillumination looks like at depths of 200, 300, and 400 m, view the figure under civil twilight, full moonlight, and half-moonlight respectively.

sis, but a bioluminescent analog of disruptive coloration. The individual photophores may break up the silhouette so that it appears as a number of small objects rather than as one large, recognizable outline. This tactic is common and highly successful in benthic and terrestrial habitats where the background is complex (Lythgoe, 1979). Its effective-

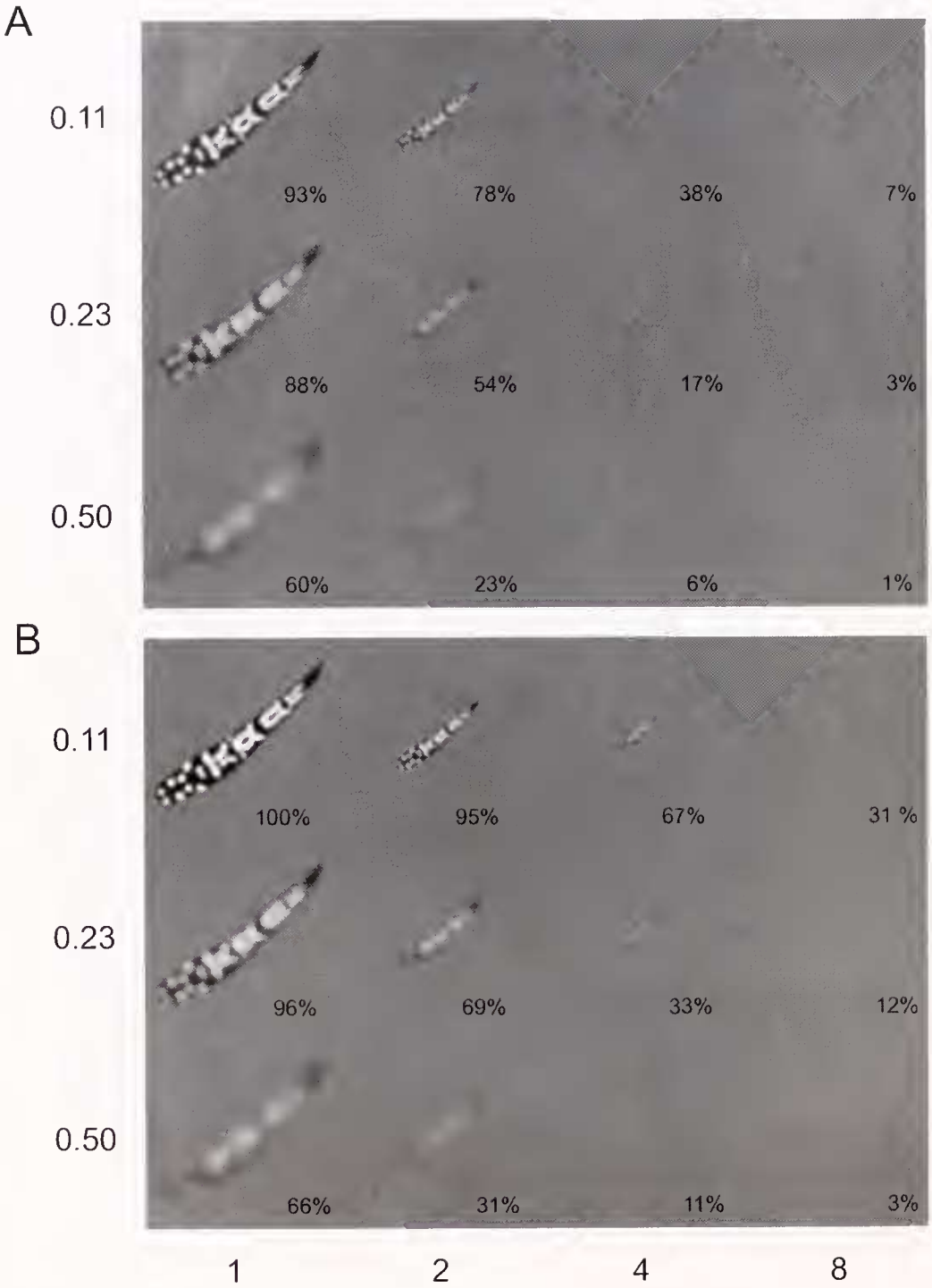

Figure 6. Identical to Figure 5, except that the counterillumination signal is generated by *Ceratoscopelus maderensis.*

ness in pelagic environments, where the background is very uniform, is uncertain. Finally, the ability of the predator to recognize the perceived image as potential prey depends on pattern recognition, a higher level of visual processing that is poorly understood in oceanic species.

Effects of intervening water on counterillumination

Despite the authors' initial expectations, the water had little effect on the appearance of the counterillumination. This was due to several factors. First, even in the worst case

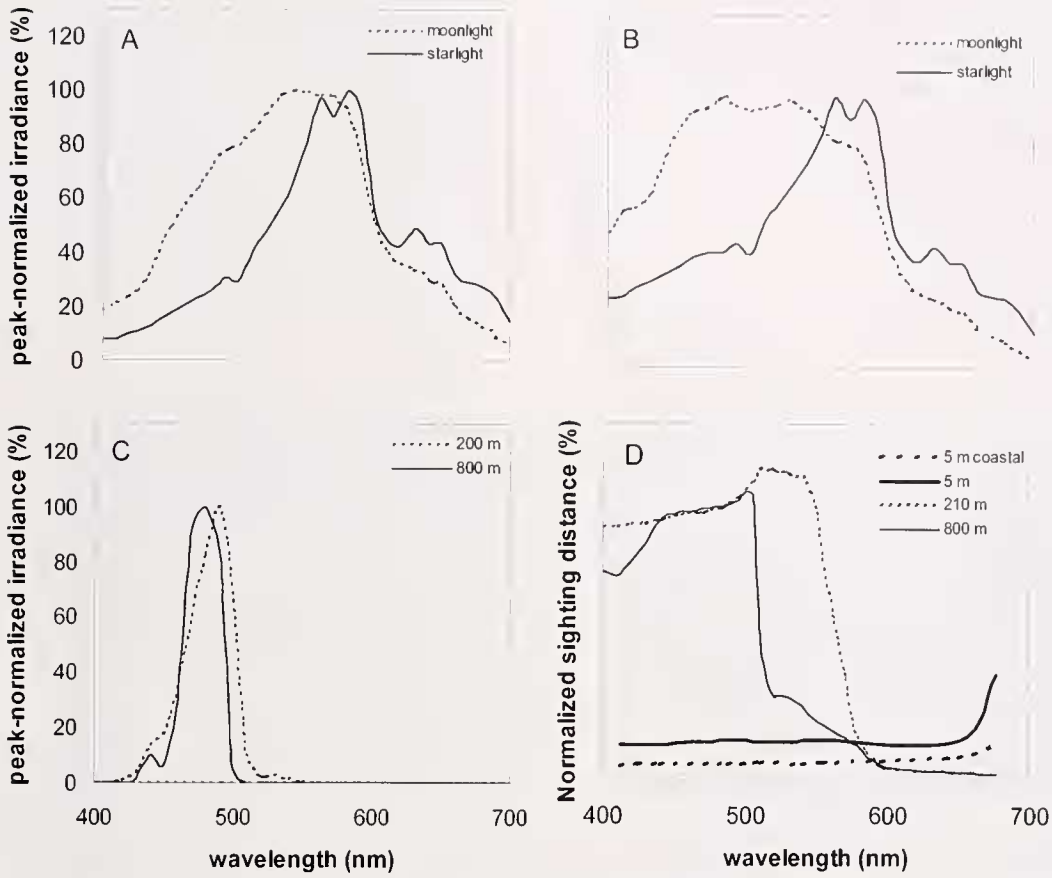

Figure 7. (A) Downwelling irradiance (normalized by peak) at 5-m depth in coastal water under moonlight and starlight. (B) Same as (A), but in oceanic water. (C) Downwelling daytime irradiance at depths of 200 and 800 m. (D) Sighting distance of a counterilluminator, normalized by sighting distance in mesopelagic waters at 480 nm. Because all published bioluminescence spectra are calibrated in energy units (instead of quanta), (A), (B) and (C) are calibrated in relative energy units.

(412-nm light in coastal water at 5-m depth), 8% of the photons were neither scattered nor absorbed after traveling 5 m ($=e^{-5(a+b)} = e^{-5(0.29+0.26)}$). The viewer perceives these uncollided photons as all arriving from one point (which has a radius determined by the spatial resolution of the eye), so the perceived radiance of this unscattered light is quite high. In contrast, the scattered photons, although more numerous (92% in this case), are scattered over a larger angular area and so have a lower radiance. Second, for a photon to contribute to image blurring, it must be scattered but not absorbed by the water. Because highly scattering waters also tend to be highly absorbing (see Table 1), many scattered photons are absorbed before they can reach the eye and thus cannot contribute to image blurring. This is in sharp contrast to atmospheric scattering (*e.g.*, due to haze or fog), which can be high while absorption is negligible (Bohren and Huffman, 1998). Finally, light scattering in water is strongly biased in the forward direction. In the phase function used in this study, more than 50% of the scattered photons are deflected less than 5° (Petzold, 1977). Thus, the halo of scattered light surrounding the image of a point source is quite narrow. This also differs from the atmospheric case, where light is often scattered over relatively large angles (Bohren and Huffman, 1998). For all the above reasons, the images in all the water types examined did not lose a substantial amount of fine detail. There are, of course, considerably more turbid marine waters (very close to shore or to river plumes, coccolithophore blooms, *etc.*). Counterilluminators, however, are seldom found in these locations.

A parameter that was greatly affected by the water was the attenuation of the contrast of the entire scene (*e.g.*, MTF(0)). The attenuation coefficient depends on the viewing angle of the predator and for upward viewing is $c - K_{Ld}$ (see Eq. 5). This coefficient is far smaller than the attenuation coefficients for viewing an object horizontally or from above (c, and $c + K_{Ld}$ respectively), so objects viewed from below are visible at much longer distances (Johnsen, 2002). This result derives from the fact that, as a viewer moves down and away from a counterilluminator, the background

dims almost as quickly as the signal does, thus maintaining the contrast. The unusual wavelength dependence of the attenuation of counterillumination occurs because c and K_{Ld} vary somewhat independently. At shorter wavelengths, $c - K_{Ld}$ increases slightly with wavelength; at longer wavelengths at depth, c increases rapidly with wavelength, while K_{Ld} remains more or less constant. This is because almost all long-wavelength light at depth is due to Raman scattering, in which a small portion of the blue-green light is converted into longer wavelength light (Marshall and Smith, 1990; Johnsen, 2002). Because this Raman-scattered light is produced *de novo* from shorter wavelength light, it has roughly the same attenuation coefficient as that light, and so the difference between c and K_{Ld} can grow quite large. But because the long wavelength light is extremely dim, it may not be of visual significance, particularly at mesopelagic depths.

A curious feature of this wavelength dependence is that the wavelength of least contrast attenuation is about 30 nm longer than the peak wavelength of the downwelling light. The lower contrast attenuation at these wavelengths allows for a slightly longer sighting distance (proportional to $1/c - K_{Ld}$: 12.5% longer at 210 m; 5.5% longer at 800 m) than at the peak wavelength. Because the spectral responses of most deep-sea visual systems are relatively flat (Douglas *et al.*, 1998), this shift may be inconsequential.

Effect of variation in background illumination

The fact that the spectrum of the background changes with depth has been examined before (*e.g.*, Young and Mencher, 1980). This study confirms that, even at mesopelagic depths, the spectrum changes substantially with depth. While a 10-nm shift in the peak wavelength appears minor, it causes large shifts in the intensity of the off-peak light because the wavelength distributions are quite narrow. For example, if the peak intensities are set equal at 100% (as in Fig. 7C), the difference between the downwelling irradiance at depths of 200 and 800 m is 62% at 500 nm and 32% at 470 nm.

A previously unconsidered issue is the effect of the nocturnal illumination source. Many counterilluminators are vertical migrators and can be found near the surface at night (the downwelling irradiance at 5-m depth under moonlight and starlight equals that found during the middle of the day at 300 and 500 m respectively). The background illumination then depends on whether the moon is present. Over a complete lunar cycle, the moon is above the horizon for about half of the nocturnal hours. Because the moon reflects all wavelengths more or less equally (Munz and McFarland, 1977), the spectrum of the night sky with the moon present is similar to the spectrum of daylight (though dimmer by about 6 orders of magnitude, and slightly red-shifted due to background starlight). When the moon is not present, the illumination has three primary components: (1) starlight, mostly due to dim red stars invisible to the naked eye, (2) scattering of sunlight by dust in the plane of the solar system, and (3) emission spectra from gases in the upper atmosphere (*e.g.*, airglow) (Munz and McFarland, 1977). The final irradiance spectrum is strongly red-shifted. Whereas the spectral shift from moonlight to starlight is minor at mesopelagic depths, it is quite obvious in near-surface waters (Fig. 7A, B), particularly in blue, oceanic waters. Since very few marine species are known to have long-wavelength sensitivity at scotopic light levels, the implications of the spectral shifts at these wavelengths are unknown. However, the shifts at blue-green wavelengths (450–500 nm) are also substantial, and can be detected by nearly all deep-sea visual systems. Although certain counterilluminating species alter the spectra of their emitted light with ambient temperature or depth (Young and Mencher, 1980; Young and Arnold, 1982; Herring *et al.*, 1992), adaptations to the spectral shift caused by the presence or absence of the moon are unknown.

Implications for counterillumination

The clarity of the water and the spectral variation due to depth and the presence or absence of the moon have several important implications for counterilluminators. First, since it is unlikely that light scattering by the water will combine the light from the individual photophores into an even light field, an animal with few, widely spaced light organs is at a disadvantage, particularly when the background light levels are relatively high. Furthermore, the fewer the photophores, the brighter they must be to balance out the unlit regions of the ventral surface. In this study, the photophores of *C. maderensis* had to be 175% brighter than the background radiance, whereas the more finely distributed photophores of *A. veranyi* had to be only 34% brighter. For this reason, a counterilluminator viewed by a high-resolution eye will appear as a signal both brighter and darker than the background (*i.e.*, bright photophores on a silhouetted body). This may explain why shallower species generally have more finely spaced photophores, since acute vision is only possible at higher levels of illumination (Widder, 1999; Warrant and Locket, 2004).

A second important implication of this study is that counterillumination is potentially more successful at shallower depths. Due to the greater contrast attenuation at shallow depths, any mismatch with the background is detectable at only 5%–20% of the distance at which the same mismatch would be detectable in deeper waters. This increase in contrast attenuation may offset the disadvantage due to the variable spectra and angular distribution found near the surface.

Finally, because contrast attenuation is relatively constant over a wide range of wavelengths (Fig. 7D), and because

contrast sensitivity decreases rather slowly with decreasing illumination (Warrant, 1999), a counterilluminator ideally must match the downwelling spectrum from about 450 to 520 nm at depth and over a somewhat greater wavelength range near the surface. However, a survey of published photophore spectra shows that this is not the case (Fig. 8). Photophores involved in counterillumination do have spectral characteristics different from those used for other purposes, but the pattern is far from intuitive. In fish, counterilluminating photophores produce light with roughly the same peak wavelength (but with a narrower spectrum) as those of non-counterilluminating photophores. In decapods, the peak is red-shifted and the spectrum narrower in counterilluminating *versus* non-counterilluminating photophores. In squid and a few fish, counterilluminating photophores emit light at a longer (and occasionally shorter) wavelength than the non-counterilluminating photophores. Interestingly, the spectra of the counterilluminators, despite being quite clustered (suggesting natural selection), seldom match the downwelling spectrum. Some are 10–20 nm too blue, and others are 10–30 nm too red. This suggests that they may be visible to predators whose color discrimination

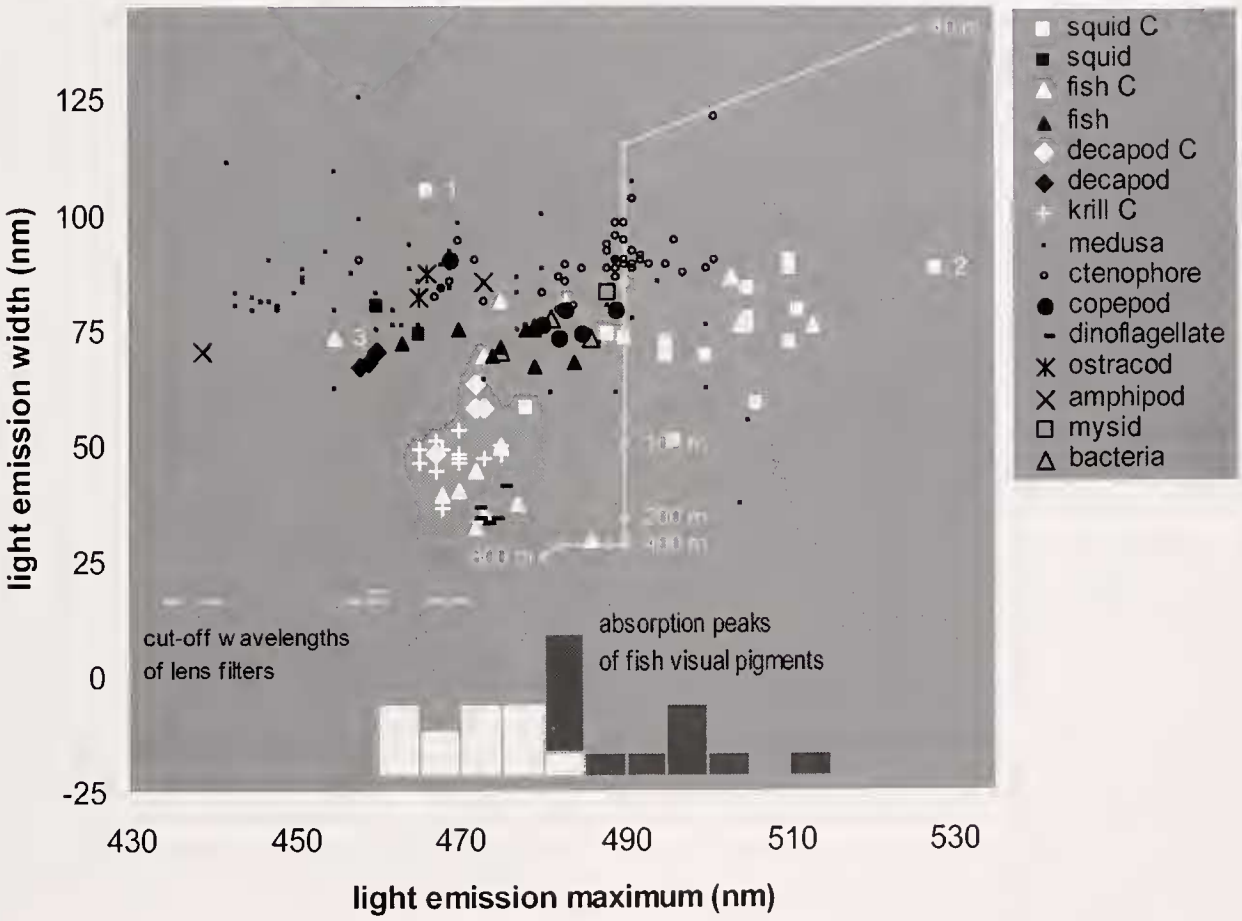

Figure 8. Peak wavelength *vs.* emission width (full-width half-max, FWHM) for the light emissions from various species. White symbols denote photophores involved in counterillumination. Black symbols denote photophores and other luminous sources used for other tasks (warning, luring, etc.). The outliers among the counterilluminators are [1]*Abraliopsis falco* (enoploteuthid squid), [2]*Teuthowenia megalops* (cranchiid squid), [3]*Isistius brasiliensis* (cookie-cutter shark). White line shows peak wavelength and FWHM for downwelling light as a function of depth (depth intervals are 10 m down to 100 m, and then 100 m for depths down to 800 m). Bar chart is a histogram of visual pigment absorption peaks for deep-sea fish eyes known to have multiple pigments in the blue-green portion of the spectrum (data from Douglas *et al.*, 1998). The white bars are the short-wavelength pigments; the black bars are the long-wavelength pigments. The gray symbols show the cut-off wavelengths for the filters in the lenses of seven species of deep-sea fish (data from Douglas and Thorpe, 1992). Photophore spectral data taken from Nicol (1960), Swift *et al.* (1973, 1977), Biggley *et al.* (1981), Herring (1983), Denton *et al.* (1985), Widder *et al.* (1983), Herring *et al.* (1992, 1993), and Haddock and Case (1999). Because the published bioluminescence spectra are calibrated in energy units (instead of quanta), the downwelling light curve is calibrated in relative energy units.

at blue and green wavelengths is good owing to multiple visual pigments or ocular filters.

Although about 15 deep-sea species (including fish, alciopid polychaetes, oplophorid shrimp, and the squid genus *Watasenia*) are known to have multiple visual pigments, most deep-sea species apparently are monochromatic, with a relatively flat spectral response near the maximum wavelength (due to the extreme thickness of their photoreceptors) (Douglas *et al.*, 1998). Therefore the spectral mismatches seen in Figure 8 may not be detectable as a color shift by many predators (excepting those possessing color filters). For a counterilluminator facing a color-blind predator, the relevant issue is that the light emitted from the photophores is attenuated more quickly than the downwelling light, due to higher absorption at non-peak wavelengths. Therefore, even if the emitted light perfectly matches the background intensity at one distance, the counterillumination will become darker than the background at a greater distance. The difference between the attenuation coefficients at 470 nm and 480 nm is small. Therefore, this issue is likely to be insignificant for the krill, fish, and decapods whose photophores emit at 470 nm. The close clustering of the spectra of these species remains puzzling, but may be an evolutionary strategy to prevent predators from developing a species-specific search image. This is analogous to the "selfish herd" effect, in which identical individuals in large aggregations reduce their chance of predation (Hamilton, 1971; Bond and Al Kamil, 2002).

The light emitted by squid photophores that peaks at 510 nm will be attenuated significantly more quickly than the downwelling light, potentially leading to the detection of the squid, but these measured spectra may not be representative of the natural spectra. As mentioned above, certain squid can change the spectrum of their counterillumination depending on temperature. Since the spectral measurements were not done *in situ* and often required a fair bit of manipulation, the squid may have been at a higher temperature and thus produced light to match shallower and therefore greener water. In fact, the published spectra of all counterilluminators must be treated with some caution because very few of the animals were measured while they were passively counterilluminating, but instead were being manually stimulated to emit light. Because manual stimulation tends to turn on all available photophores in an attention-getting signal that is assumed to act as a "burglar alarm" (Widder, 1999), the measured spectrum may include light from photophores that are not active during counterillumination, altering the spectrum.

Effects of visual resolution and color discrimination on perceived image

Although the range of water types commonly inhabited by counterilluminators had little effect on their visibility, the range of visual acuities of potential predators had a dramatic effect. Because light scattering by the water had little effect on the appearance of the counterillumination signal, acute vision can detect the individual photophores and is therefore highly advantageous. Indeed, many deep-sea species are known to have far greater resolution ($\sim 10\times$) in the dorsal viewing region than in other directions (Collin *et al.*, 1997; Wagner *et al.*, 1998; Land, 1999; Warrant and Locket, 2004). For example, although the spatial resolution for upward viewing in the hatchet fish *Argyropelecus aculeatus* is 0.11° (see Materials and Methods), the spatial resolution over the rest of visual field is 0.7°–1.7° (Collin *et al.*, 1997). In contrast, the myctophid *Lampanyctus festivus*, which has lateral-viewing eyes, has a relatively constant and low visual acuity (0.5°) over the entire visual field (Wagner *et al.*, 1998). Because this increased spatial resolution decreases sensitivity (and hence ability to detect contrast), it has an associated cost. Warrant and Locket (2004) analyzed the benefits and costs of high spatial resolution as a function of what is being viewed; they determined that high spatial resolution should be selected for in eyes that search overhead for small, silhouetted objects. While they do not explicitly consider the spatial pattern of counterillumination, the same principles apply.

The high spectral variation of the background light and the spectral mismatches seen in Figure 8 suggest that good color discrimination in the blue-green would be extremely advantageous. As mentioned above, certain deep-sea species probably have good color discrimination at blue and green wavelengths. Indeed, the peaks of these pigments seem to support the hypothesis of Douglas *et al.* (1998) that one pigment matches the counterilluminator's spectrum and one matches the downwelling light (Fig. 8). In addition, certain species with only one visual pigment have multibanked retinas. The filtering of the light by the vitread banks alters the spectrum of the light reaching the sclerad banks, changing their sensitivity and theoretically allowing for color discrimination (Denton and Locket, 1989). Finally, the lenses of certain deep-sea species have yellow filters that can also increase the contrast of a counterilluminator against the background (Munz, 1976; Douglas and Thorpe, 1992).

Conclusions

Although counterillumination is a ubiquitous and successful cryptic strategy, the clarity of the water implies that the camouflage can be broken by species with acute vision at longer distances than anticipated. In addition, the background to be matched depends not only on depth, but also on the source of nocturnal illumination. While spectral variation is greatest near the surface, contrast attenuation is also greatest. These results suggest several fruitful avenues for future research, including further analysis of the conflicting constraints of visual sensitivity and spatial resolu-

tion, a determination of how counterilluminators that can change spectral emissions choose the correct spectrum (despite being color-blind), and investigation of a possible relationship between the resolution of ventral photophore patterns and the acuity of potential predators.

Acknowledgments

The authors thank Drs. Eric Warrant, Tamara Frank, Steven Haddock, Richard Young, Roger Hanlon, and Peter Herring for a critical reading of earlier versions of the manuscript, and Drs. Craig Bohren, Jules Jaffe, Robert Maffione, Ken Voss, and Ron Zaneveld for helpful discussions. This work was funded in part by grants from the Office of Naval Research to EAW and SJ (N00014-02-1-0949) and to CDM. This is contribution number 1557 of the Harbor Branch Oceanographic Institution.

Literature Cited

Anthony, P. D. 1981. Visual contrast thresholds in the cod *Gadus morhua*. *J. Fish Biol.* **19:** 87–103.

Biggley, W. H., T. Napora, and E. Swift. 1981. The color of bioluminescent secretions from decapod prawns in the genera *Oplophorus* and *Systellaspis* (Caridea). Pp. 66–71 in *Bioluminescence: Current Perspectives*, K. H. Nealson, ed. Burgess Publishing, Minneapolis, MN.

Bogucki, D. J., J. A. Domaradzki, D. Stramski, and J. R. Zaneveld. 1998. Comparison of near-forward scattering on oceanic turbulence and particles. *Appl. Optics* **37:** 4669–4671.

Bohren, C. F., and D. R. Huffman. 1998. *Absorption and Scattering by Small Particles.* John Wiley & Sons, New York.

Bond, A. B., and A. C. Kamil 2002. Visual predators select for crypticity and polymorphism in virtual prey. *Nature* **415:** 609–613.

Capone, A., T. Digaetano, A. Grimaldi, R. Habel, D. Lo Presti, E. Migneco, R. Masullo, F. Moro, M. Petruccetti, C. Petta, P. Piatelli, N. Randazzo, G. Riccobene, E. Salusti, P. Sapienza, M. Sedita, L. Trasatti, and L. Ursella. 2002. Measurements of light transmission in deep sea with the AC9 transmissometer. *Nucl. Instr. Meth. Phys. Res.* **487:** 423–434.

Collin, S. P., R. V. Hoskins, and J. C. Partridge. 1997. Tubular eyes of deep-sea fishes: a comparative study of retinal topography. *Brain Behav. Evol.* **50:** 335–357.

Denton, E. J., and N. A. Locket. 1989. Possible wavelength discrimination by multibank retinae in deep-sea fishes. *J. Mar. Biol. Assoc. UK* **69:** 409–435.

Denton, E. J., J. B. Gilpin-Brown, and P. G. Wright. 1972. The angular distribution of the light produced by some mesopelagic fish in relation to their camouflage. *Proc. R. Soc. Lond. B* **182:** 145–158.

Denton, E. J., P. J. Herring, E. A. Widder, M. F. Latz, and J. F. Case. 1985. The roles of filters in the photophores of oceanic animals and their relation to vision in the oceanic environment. *Proc. R. Soc. Lond. B* **225:** 63–97.

Douglas, R. H., and C. W. Hawryshyn. 1990. Behavioral studies of fish vision: an analysis of visual capabilities. Pp. 373–418 in *The Visual System of Fish*, R. H. Douglas and M. B. A. Djamgoz, eds. Chapman and Hall, New York.

Douglas, R. H., and A. Thorpe. 1992. Short-wave absorbing pigments in the ocular lenses of deep-sea teleosts. *J. Mar. Biol. Assoc. UK* **72:** 93–112.

Douglas, R. H., J. C. Partridge, and N. J. Marshall. 1998. The eyes of deep-sea fish. I. Lens pigmentation, tapeta and visual pigments. *Prog. Retin. Eye Res.* **17:** 597–636.

Frank, T. M. 1999. Comparative study of temporal resolution in the visual systems of mesopelagic crustaceans. *Biol. Bull.* **196:** 137–144.

Goodman, J. W. 1996. *Introduction to Fourier Optics.* McGraw Hill, New York.

Haddock, S. H. D., and J. F. Case. 1999. Bioluminescence spectra of shallow and deep-sea gelatinous zooplankton: ctenophores, medusae, and siphonophores. *Mar. Biol.* **133:** 571–582.

Hamilton, W. D. 1971. Geometry for the selfish herd. *J. Theor. Biol.* **31:** 295–311.

Harper, R. D., and J. F. Case. 1999. Disruptive counterillumination and its anti-predatory value in the plainfish midshipman *Porichthys notatus*. *Mar. Biol.* **134:** 529–540.

Herring, P. J. 1977. Luminescence in cephalopods and fish. *Symp. Zool. Soc. Lond.* **38:** 127–159.

Herring, P. J. 1983. The spectral characteristics of luminous marine organisms. *Proc. R. Soc. Lond. B* **220:** 183–217.

Herring, P. J. 1985. Bioluminescence in the crustacea. *J. Crustac. Biol.* **5(4):** 557–573.

Herring, P. J., E. A. Widder, and S. H. D. Haddock. 1992. Correlation of bioluminescence emissions with ventral photophores in the mesopelagic squid *Abralia veranyi* (Cephalopoda: Enoploteuthidae). *Mar. Biol.* **112:** 293–298.

Herring, P. J., M. I. Latz, N. J. Bannister, and E. A. Widder. 1993. Bioluminescence of the poecilostomatoid copepod *Oncaea conifera*. *Mar. Ecol. Prog. Ser.* **94:** 297–309.

Jaffe, J. S. 1992. Validity and range of linear approximations in underwater imaging. Pp. 388–396 in *Ocean Optics XII*, G. D. Gilbert, ed. The International Society of Optical Engineering, Bellingham, WA.

Johnsen, S. 2002. Cryptic and conspicuous coloration in the pelagic environment. *Proc. R. Soc. Lond. B* **269:** 243–256.

Johnsen, S., and H. M. Sosik. 2003. Cryptic coloration and mirrored sides as camouflage strategies in near-surface pelagic habitats: implications for foraging and predator avoidance. *Limnol. Oceanogr.* **48:** 1277–1288.

Land, M. F. 1999. Compound eye structure: matching eye to environment. Pp. 51–71 in *Adaptive Mechanisms in the Ecology of Vision*, S. N. Archer, M. B. A. Djamgoz, E. R. Loew, J. C. Partridge, and S. Vallerga, eds. Kluwer Academic, Boston.

Latz, M. I. 1995. Physiological mechanisms in the control of bioluminescent countershading in a midwater shrimp. *Mar. Freshw. Behav. Physiol.* **26:** 207–218.

Lythgoe, J. N. 1979. *The Ecology of Vision.* Clarendon Press, Oxford.

Marshall, B. R., and R. C. Smith. 1990. Raman scattering and in-water optical properties. *Appl. Optics* **29:** 71–84.

Mertens, L. E. 1970. *In-Water Photography: Theory and Practice.* John Wiley, New York.

Mertens, L. E., and R. S. Replogle. 1977. Use of point spread and beam spread functions for analysis of imaging systems in water. *J. Opt. Soc. Am.* **67:** 1105–1117.

Mobley, C. D. 1994. *Light and Water: Radiative Transfer in Natural Waters.* Academic Press, New York.

Mobley, C. D., B. Gentili, H. R. Gordon, Z. Jin, G. W. Kattawar, A. Morel, P. Reinersman, K. Stamnes, and R. H. Stavn. 1993. Comparison of numerical models for computing underwater light fields. *Appl. Optics* **32:** 7484–7504.

Munz, W. R. A. 1976. On yellow lenses in mesopelagic animals. *J. Mar. Biol. Assoc. UK* **56:** 963–976.

Munz, F. W., and W. N. McFarland. 1977. Evolutionary adaptations of fishes to the photic environment. Pp. 194–274 in *The Visual System of Vertebrates*, F. Crescitelli, ed. Springer-Verlag, New York.

Nicol, J. A. C. 1960. Spectral composition of the light of the lantern-fish, *Myctophum punctatum. J. Mar. Biol. Assoc. UK* **39:** 27–32.

Petzold T. J. 1977. Volume scattering functions for selected ocean waters. Pp. 150–174 in *Light in the Sea.* J. E. Tyler, ed. Dowden, Hutchinson, and Ross, Stroudsberg, PA.

Swift, E., W. H. Biggley, and H. H. Seliger. 1973. Species of oceanic dinoflagellates in the genera *Dissodinium* and *Pyrocystis:* interclonal and interspecific comparisons of the color and photon yield of bioluminescence. *J. Phycol.* **9:** 420–426.

Swift, E., W. H. Biggley, and T. Napora. 1977. The bioluminescence emission spectra of *Pyrosoma atlanticum, P. spinosum* (Tunicata), *Euphausia tenera* (Crustacea) and *Gonostoma sp.* (Pisces). *J. Mar. Biol. Assoc. UK* **57:** 817–823.

Ulloa, O., S. Sathyendranath, and T. Platt. 1994. Effect of the particle-size distribution on the backscattering ratio in seawater. *Appl. Optics* **33:** 7070–7077.

Vecchione, M., and C. F. E. Roper. 1991. Cephalopods observed from submersibles in the western north Atlantic. *Bull. Mar. Sci.* **49:** 433–445.

Voss, K. J. 1991. Simple empirical model of the oceanic point spread function. *Appl. Optics* **30:** 2647–2651.

Wagner, H. J., E. Froehlich, K. Negishi, and S. P. Collin. 1998. The eyes of deep-sea fish II. Functional morphology of the retina. *Prog. Retin. Eye Res.* **17:** 637–685.

Warrant, E. J. 1999. Seeing better at night: life style, eye design, and the optimum strategy of spatial and temporal summation. *Vision Res.* **39:** 1611–1630.

Warrant, E. J., and N. A. Locket. 2004. Vision in the deep sea. *Biol. Rev. Camb. Philos. Soc.* (In press).

Widder, E. A. 1999. Bioluminescence. Pp. 555–581 in *Adaptive Mechanisms in the Ecology of Vision,* S. N. Archer, M. B. A. Djamgoz, E. R. Loew, J. C. Partridge, and S. Vallerga, eds. Kluwer Academic, Boston.

Widder, E. A., M. I. Latz, and J. F. Case. 1983. Marine bioluminescence spectra measured with an optical multichannel detection system. *Biol. Bull.* **165:** 791–810.

Young, R. E., and J. M. Arnold. 1982. The functional morphology of a ventral photophore from the mesopelagic squid, *Abralia trigonura. Malacologia* **23:** 135–163.

Young, R. E., and F. M. Mencher. 1980. Bioluminescence in mesopelagic squid: diel color change during counterillumination. *Science* **208:** 1286–1288.

Young, R. E., and C. F. E. Roper. 1976. Bioluminescent countershading in midwater animals: evidence from living squid. *Science* **191:** 1046–1048.